Please cite instead:

Leclercq, L., Marczak, F., Knoop, V.L., and Hoogendoorn, S.P. (2016) Capacity Drops at Merges: Analytical Expressions for Multilane Freeways. Accepted for Transportation Research Records; DOI is 10.3141/2560-01

Capacity drops at merges: analytical expressions for multilane freeways

Ludovic Leclercq (Corresponding author)
Professor
Université de Lyon, Lyon, France
IFSTTAR, COSYS-LICIT, Bron, France
ENTPE, LICIT, Vaulx-en-Velin, France
ludovic.leclercq@entpe.fr

Florian Marczak
Research Engineer, PhD
DREAL-Alsace, Strasbourg, France
florian.marczak@developpement-durable.gouv.fr

Victor L. Knoop
Assistant Professor
Delft University of Technology
Stevinweg 1
Delft, The Netherlands
v.l.knoop@tudelft.nl

Serge P. Hoogendoorn
Professor
Delft University of Technology
Stevinweg 1
Delft, The Netherlands
s.p.hoogendoorn@tudelft.nl

Paper submitted for presentation to
the 95th meeting of the *Transportation Research Board*
and publication *to Transportation Research Record*

Submission date:
Paper number: 16-00xx
5404 Words + 5 figures = 6654 words (excluding references)

Abstract

This paper deals with the derivation of analytical formulae to estimate the effective capacity at freeway merges in a multilane context. It extends two previous papers that are based on the same modeling framework but that are restricted to a single lane on the freeway (or to the analysis of the right lane only). The analytical expression for the one-lane capacity is recursively applied for all lanes. Lane-changing maneuvers (mandatory for the on-ramp vehicles and discretionary for others) are partitioned into two non-overlapping local merging areas. Discretionary lane-changes are transformed into a lane-changing flow using an appropriate analytical formula. This defines a system of equations whose unknowns are the capacity on all lanes and the inserting flow coming from the on-ramp. A sensitivity analysis shows that vehicle acceleration and the truck ratio are the most influential parameters for the total capacity. The analytical formulae are proven to match with numerical results from a traffic simulator that fully describes vehicle dynamics. Finally, they provide very good estimates when compared to experimental data for an active merge on the M6 freeway in UK.

Introduction

Two key figures to describe merges on freeway are the merge ratio and the effective capacity. The merge ratio represents how the incoming flows share the downstream effective capacity in congestion (1)-(3). Experimental evidences for lots of different locations demonstrate that this ratio is fixed whatever the downstream flow value is (3)-(6). The effective capacity corresponds to the maximum flow that can be observed downstream of congested merges. It is observed when downstream traffic conditions are free-flow and so the merge acts as an active bottleneck. Effective capacity is also referred in some papers, e.g. (7)-(8), as the queue discharge rate because the congestion head is located close to the merge. Experimental findings show that the effective capacity is classically below the maximal observed flow in free-flow with a magnitude between 10 to 30%, e.g. (8)-(16). Several physical explanations have been proposed in the literature to explain such a capacity drop: merging vehicles that insert at lower speeds and need times to accelerate, e.g. (17)-(20), impacts of different driver behaviors or car characteristics, e.g. (5), (7), (21), (22), lane changes and the global acceleration process that happens downstream of the merge, e.g. (23)-(25). Most of these explanations involve acceleration patterns with slower vehicles that create local voids in front of them that temporally reduce the flow.

Except for direct experimental observations, the most common way to determine the effective merge capacity is to use a traffic model able to reproduce the underlying physical mechanisms, e.g. (15)-(20). This requires running a simulation for every new set of parameters and is not really convenient when looking for a first and quick approximation of how a merge behaves. To the authors knowledge, (26) is the first to propose a different approach based on analytical considerations. The main source of the capacity drop is supposed to be the inserting vehicles. These vehicles are considering to act as moving bottlenecks (27), (28) with a bounded acceleration while mainstream vehicles are reproduced by the kinematic wave theory (29), (30) with a triangular fundamental diagram. (26) provides an implicit analytical expression that defines the effective capacity of a congested merge with respect to the fundamental diagram parameters, the value of the acceleration, the merge ratio and the length of the on-ramp. This first attempt has three main shortcomings. First, the application of the kinematic wave theory was over-simplified and does not consider the interactions between downstream congestion waves and voids that appear in front of inserting vehicles (moving bottlenecks). Second, vehicles characteristics and especially their acceleration rate and their size (jam density) are supposed homogeneous. Third, the analytical derivations are only provided for one-lane freeway. Extensions to multilane cases are discussed in (26) but the authors were only able to define very simple method that provides large bounds and not a direct value for the total effective capacity.

Recently, (31) proposes new analytical investigations in line with the previous framework. This permits to eliminate the two first shortcomings. First, the interactions between waves and voids were properly handled and integrate in a refined implicit analytical expression. It appears that the capacity value increases by 15 to 20% when such interactions are considered for the same parameter settings. This is because waves are delayed by voids, which increases the available capacity. Second, heterogeneous vehicles characteristics have been introduced. Now, acceleration rate for inserting vehicles can be distributed as so the jam density to distinguish the effects of cars and trucks. The main conclusion for this second extension is that considering the distribution of these parameters has little impacts on the mean effective capacity as long as the mean value of each parameter is properly estimated.

The current paper entirely focuses on the last shortcoming, i.e. the multilane extension. This implies to consider not only mandatory lane changes that correspond to inserting vehicles but also discretionary lane changes that correspond to vehicles that want to avoid the inserting area. A global framework is proposed to determine the effective capacity for all freeway lanes while accounting for both these phenomenon. This leads to an implicit and well-defined system of equations whose solutions provide the local capacity on all lanes and the inserting flow when the merge is an active bottleneck. The global analytical model will be compared to outputs from a classical traffic simulator and to experimental data to demonstrate its performance.

This paper is organized as follow: section 1 presents the global modeling framework. Section 2 focuses on numerical investigations with both a sensitivity analysis and a comparison with simulation outputs. Section 3 provides a first experimental validation on the same experimental site as in (26). This notably shows that the new framework leads to analytical estimates that are very close to observations while the original works only provides very large bounds. Section 4 presents a brief conclusion.

1. The modeling framework

In this section, we present the modeling framework for a two-lane freeway. Extension to higher lane numbers can be obtained in a recursive manner as presented in section 3 for a three-lane freeway.

Partitioning a multilane merge in different local merges

(17) derives from experimental observations a complete description of the physical mechanisms that can be observed at a congested freeway merge. First, inserting vehicles that realize mandatory lane changes tend to reduce the average speed on the right lane when they become too numerous, see area 1 in Fig. 1a. This is the primary cause for the capacity drop. Then, vehicles from the freeway try to avoid the speed reduction on the right lane by moving to the left lane, see area 2 in Fig. 1a. Such discretionary lane changes start happening at lower speed when the congestion is well established on the right lane. Thus, the capacity reduction spreads over the other lane because of the lane-changing process. At the end, all the lanes experiment congested traffic states and the exit flow from the bottleneck corresponds to the effective capacity. Discretionary lane changes can also be observed downstream of the inserting area but they are not numerous and do not really influence the capacity value, see area 3 in Fig1. a.

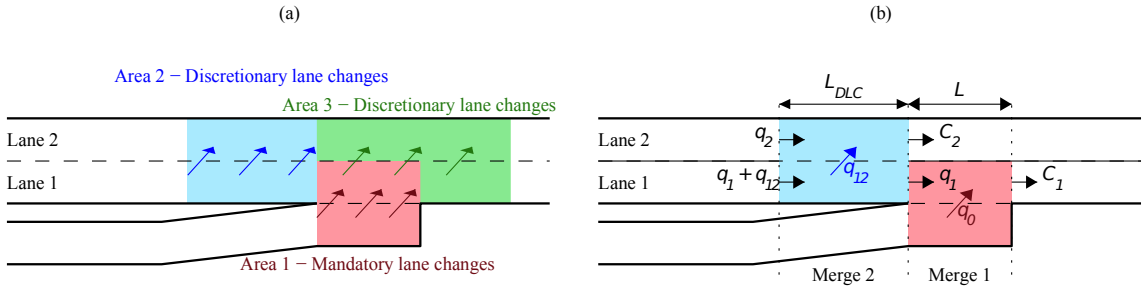

Figure 1: Sketch of a multilane merge (a) the different lane-changing maneuvers (b) spatial partitioning and notations

To derive analytical formulation of the effective capacity of a multilane merge, we have to simplify the physical process. In particular, we need to partition the different lane-changing maneuvers into several non-overlapping spatial areas. Otherwise, it would be too difficult to analytically resort to the

conservation principle per lane because lateral flows would be observed on both lane sides. Fortunately, such a spatial partitioning is consistent with the physical mechanisms described in (17). Here, we assume that the discretionary lane changes from lane 1 to lane 2 happen first in an area located just upstream of the on-ramp, i.e. the blue area in Fig. 1b. The length of this area is denoted L_{DLC}. The mandatory lane changes from the on-ramp to 1 then happen in the red area in Fig. 1b. The length of the inserting area is L. Both areas (blue and red) are consecutive with no overlapping. They define a spatial partition corresponding to two consecutive merges, i.e. merges 2 and 1 in Fig. 1b. When all lane are congested, the exit flow from lane 2 (respectively lane 1) corresponds to the effective capacity C_2 of lane 2 (respectively C_1 of lane 1). Let denote q_0 and q_{12} the inserting flows and q_1 and q_2 the main inflows for merges 1 and 2, see Fig 1b. It results that:

$$\begin{cases} q_0+q_1=C_1(\text{merge } 1) \\ q_{12}+q_2=C_2(\text{merge } 2) \end{cases} \quad \text{Eq. (1)}$$

This formal representation neglects the discretionary lane-changing that can be observed downstream of the on-ramp, see area 3 in Fig. 1a. As previously mentioned, such lane changes are not numerous compared to those that occur in area 1 and 2. Furthermore, their contribution to the capacity drop is low because most of the flow obstructions appear upstream of the on-ramp. This means that lane changes in area 3 benefit from voids created upstream. So we claim that this hypothesis has limited impacts on the calculation of the effective capacity for all lanes. This will be supported by the results of the experimental investigations in section 3.

Finally, we can notice that merge 1 corresponds to the usual merging process that can be represented by the well-known Daganzo's merge model (2). Let denote α_l the local merge ratio between the on-ramp and lane 1.

$$\alpha_l=\frac{q_0}{q_1}^{\text{merge 1)}} \quad \text{Eq. (2)}$$

Here, the definition for the merge ratio α_l is not classical because the denominator does not correspond to total inflow for all freeway lanes as presented in (2) and (3). We denote the global merge ratio α_g when the total inflow is used as the denominator. Interestingly, α_g can simply be deduced in our modeling framework from all the system variables (flow values), i.e. $\alpha_g=q_0/(q_1+C_2)$, see Fig 1b. It would have been possible to directly use the global merge ratio α_g to define our system of equations but we decided to set the model parameters at the level of the local merges.

Analytical expression of the effective capacity for a given inserting flow

The previous decomposition of a multilane merge into two non-overlapping local merges greatly simplify the analytical investigations. Each merge has only one targeted lane for the insertions. The analytical expressions for the effective capacity C_1 and C_2 with respect to the related inserting flows q_0 and q_{12} can then directly be derived from the analytical formulae provided in (26) and (31). It is out-of-the-scope of this paper to explain how these formulae can be derived. We will only recall the main hypothesis and provide the formulation when vehicle characteristics are homogeneous. The readers are particularly referred to (31) and (34) for details and extension to the heterogeneous case.

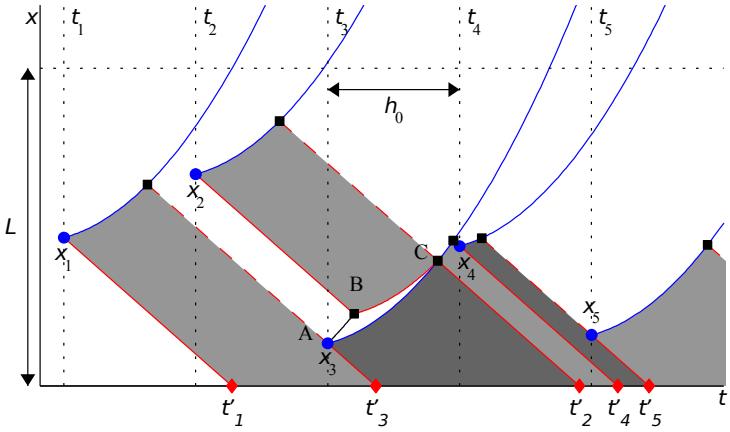

Figure 2: Deriving the analytical expression of the effective capacity for the targeted lane

Fig 2 presents how the analytical expression for the effective capacity can be derived using merge 1 as an example. Vehicle i inserts at time t_i at location x_i that is uniformly distributed over L. The time lapse h_0 between two insertions depends on the inserting flow, i.e. $h_0=1/q_0$. Inserting vehicles are considered as moving bottlenecks (27), (28) on the targeted lane with initial speed v_0 and bounded acceleration a. Platoons of vehicles upstream of each moving bottleneck are described by the kinematic wave theory (29), (30) and a triangular fundamental diagram with wave speed w and jam density κ. Free-flow speed has no influence because we only focus on congested traffic states.

Each inserting vehicles generate a traffic wave that propagate backward at speed w until it reaches the origin of the on-ramp, i.e. x=0. Such wave can reach x=0 without perturbations, e.g. vehicle 1 in Fig. 2, but can also meet a void downstream of an accelerating vehicle, e.g. the wave from vehicle 2 meets the void created by vehicle 3 in Fig. 2. In that latter case, the wave is delayed until the void disappears and arrives latter at x=0. The mean capacity value can be calculated at any location because the flow is conservative. At x=0, it appears that the flow evolution is composed with repetitive patterns that start again every time a wave crosses x=0. The tenets of the variational theory (33) make it possible to derive the long-term mean capacity value C_1 by separately calculating the mean flow values for each pattern:

$$C_1=\frac{w\kappa}{h_0}\left(h_0-T(h_0)+\frac{1}{2}s^2\frac{a\,w^2}{\gamma^3(h_0)}-\frac{1}{2}c^2\frac{2w\,h_0}{\gamma^3(h_0)}\right)$$

$$\text{with } \gamma(h_0)=\sqrt{(w+v_0)^2+2awh_0};\ T(h_0)=\frac{\left(-w-v_0+\gamma(h_0)\right)}{a}$$

$$s^2=\begin{cases}\dfrac{L^2}{6w^2}\ if\ L\le w\,h_0\\ h_0^2\left(\dfrac{\left(L-\frac{w\,h_0}{\sqrt{6}}\right)}{\left(L+\left(\sqrt{6}-2\right)w\,h_0\right)}\right)^2\ if\ L>w\,h_0\end{cases} \qquad \text{Eq. (3)}$$

$$\int ¿\left(T(h_0)-\frac{1}{2}s^2\frac{a\,w^2}{\gamma^3(h_0)}\right)+a\left(T^2(h_0)+\frac{1}{2}s^2\frac{2w^2(w+v_0)}{\gamma^3(h_0)}\right)$$

$$c^2=2a\,p_¿$$

p_{int} is the probability for a wave created by a vehicle to meet a void before reaching x=0. Its analytical expression is provided by Eq.(6) and Eq.(7) in (31). (31) also provides extended formulation to consider heterogeneous vehicle characteristics. This notably permits to distribute vehicle behaviors and more particularly to distinguish cars and trucks with different mean jam density (κ_c and κ_t) and mean acceleration capabilities (a_c and a_t). In that case, the fraction of trucks is denoted p.

Finally, it appears that C_1 and C_2 can be respectively expressed as a function of q_0 and q_{12}. The initial speeds v_0 and v_1 for the inserting vehicles at merges 1 and 2 respectively are derived from the flow value observed on the origin lane using the fundamental diagram. Thus, Eq.(1) can be refined and combined with Eq.(2) to obtain:

$$\begin{cases} q_0+q_1=C_1(q_0,v_0) \text{ with } v_0=\dfrac{w\,q_0}{(w\kappa-q_0)} \text{ (merge 1)} \\ q_1=q_0/\alpha_l \text{ (merge 1)} \\ q_{12}+q_2=C_2(q_{12},v_1) \text{ with } v_1=\dfrac{w(q_1+q_{12})}{(w\kappa-q_1-q_{12})} \text{ (merge 2)} \end{cases} \quad \text{Eq. (4)}$$

The system defined by Eq.(4) has four unknowns, i.e. q_0, q_{12}, q_1 and q_2 but only three equations. Note that if we apply the general expressions provided in (31) for calculating C_1 and C_2 the involved parameters are:

- wave speed, w,
- truck fraction, p,
- mean values for car and trucks accelerations, a_c and a_t,
- standard deviations for car and truck accelerations, $s_{a,c}$ and $s_{a,t}$,
- mean values for car and truck jam densities, κ_c and κ_t,
- standard deviations for car and truck jam densities, $s_{\kappa,c}$ *and* $s_{\kappa,t}$.

Analytical expression for discretionary lane changes and merge 2

A fourth equation can be added to the previous system by focusing on the lane-changing flow related to merge 2. (32) describes a simple but continuous lane-changing model for discretionary maneuvers. The analytic expression of the macroscopic lane-changing rate Φ per unit of space is given by:

$$\phi(k_i,k_j)=min\left(1,\frac{\mu(k_j)}{\lambda(k_j)}\right)\lambda(k_i)\frac{max(v_j-v_i,0)}{u^2\tau} \quad \text{Eq. (5)}$$

where k_i and k_j are respectively the densities on the origin and the targeted lanes, v_i and v_j the speeds on the origin and the targeted lanes, λ the demand function, i.e $\lambda(k)$=min(uk,$uw\kappa/(w+\kappa)$), μ the supply function, i.e. $\mu(k)$=min($uw\kappa/(w+\kappa)$,$w(\kappa-k)$), u the free-flow speed and τ a parameter that represents the duration of a lane-changing maneuver.

Here, we focus on situations where both lanes 1 and 2 are congested. Both demand functions then reduce to the maximal capacity. The supply on lane 2 can be approximated by the outflow, i.e. C_2. Thus, Eq.(5) becomes:

$$\phi(k_i,k_j)=C_2\frac{max(v_2-v_1,0)}{u^2\tau} \quad \text{Eq. (6)}$$

Finally, the lane-changing flow q_{12} can be determined by integrating Φ over the spatial extend of merge 2. It comes that:

$$q_{12} = C_2 \frac{max(v_2 - v_1, 0)}{u^2 \tau} L_{DLC} \quad \text{Eq. (7)}$$

The speed v_2 can be derived from the flow on lane 2 using the fundamental diagram. At the end, we succeed to define a system of 4 equations and 4 unknowns for a merge with two-lane on the freeway and one-lane on the on-ramp, see Eq.(8). The numerical solutions can be easily computed using a classical solver like in (26) or (35). Note that the total effective capacity C is equal to C_1+C_2 but also to $q_0+q_1+q_{12}+q_2$.

$$\begin{cases} q_0 + q_1 = C_1(q_0, v_0) \text{ with } v_0 = \dfrac{w\, q_0}{(w\kappa - q_0)} \text{ (merge 1)} \\ q_1 = q_0 / \alpha_l \text{ (merge 1)} \\ q_{12} + q_2 = C_2(q_{12}, v_1) \text{ with } v_1 = \dfrac{w(q_1 + q_{12})}{(w\kappa - q_1 - q_{12})} \text{ (merge 2)} \\ q_{12} = C_2 \dfrac{max(v_2 - v_1, 0)}{u^2 \tau} L_{DLC} \text{ with } v_2 = \dfrac{w\, q_2}{(w\kappa - q_2)} \text{ (merge2)} \end{cases} \quad \text{Eq. (8)}$$

2. Numerical investigations

In this section, we are first going to perform a sensitivity analysis to identify the most influential parameters on the effective capacities per lanes and the total effective capacity. Then, the analytical model will be compared with numerical results provided by a microscopic traffic simulator. Such a simulator provides a refined description of lane-changing maneuvers and the related traffic dynamics. This will permit to test the relevance of the analytical model as a first approximation for the effective capacity values.

Sensitivity analysis

We first define a reference scenario for the two-lane freeway with the following parameters: L=150 m, L_{DLC}=100 m, α_l=1, τ=1.3 s, p=15 %, a_c=2 m.s^{-2}, a_l=1 m.s^{-2}, $s_{a,c}$=0 m.s^{-2}, $s_{a,l}$=0 m.s^{-2}, κ_c=0.145 veh/m and κ_l=0.067 veh/m, $s_{\kappa,c}$=0 veh/m and $s_{\kappa,l}$=0 veh/m, w=5.38 m.s^{-1}, u=31.9 m.s^{-1}. Fig. 3 presents the results of the sensitivity analysis for the first seven parameters. In all cases, C_1 appears to be lower than C_2. This corresponds to our expectation because the capacity restriction related to low-speed vehicle insertions is supposed to be maximal close to the on-ramp. Fig. 3a shows that the length of the on-ramp influences the effective capacity on lane 1 only when L is below 150 m. C_1 reduces from 0.39 veh/s to 0.35 veh/s (-10%) when L is cut from 150 m to 50 m. L has no influence on C_2. This is not surprising considering the modeling framework we propose because inserting vehicles from the on-ramp are not allowed to change lane again. On the contrary, the length of the discretionary lane-changing area only influences C_2, see Fig. 3b. The variations are quite small with no more than 6% between the lowest C_2 value when L_{DLC}=80 m and the highest C_2 value when L_{DLC}=300 m. C_2 is slightly increasing when L_{DLC} is increasing. This should result of the combination of two effects: the lane-changing flow should increase because more space is available for the lane-changing maneuvers but the initial speed should be higher which limits the impact of inserting vehicles on lane 2.

Fig. 3c confirms an important result already highlighted in (26): the local merge ratio has almost no influence on C_1. Higher merge ratio means higher inserting flow and so higher speed on the on-ramp while lower merge ratio means lower inserting flow but also lower speed. In the latter case, few insertions are observed but they individually create stronger capacity reduction. This is remarkable that both effects compensate when the local merge ratio changes. Here, we can go further in the analysis by studying the effect on lane 2. It comes that C_2 is higher for lowest α_l values. C_2 varies from 0.47 veh/s to 0.43 veh/s when α_l increases from 0.5 to 1.5. Lower α_l values mean lower inserting flow and higher flow upstream of the on-ramp on lane 1. Thus, the initial speed for discretionary lane changes is higher, which should reduce the influence of lane-changing maneuvers on lane 2.

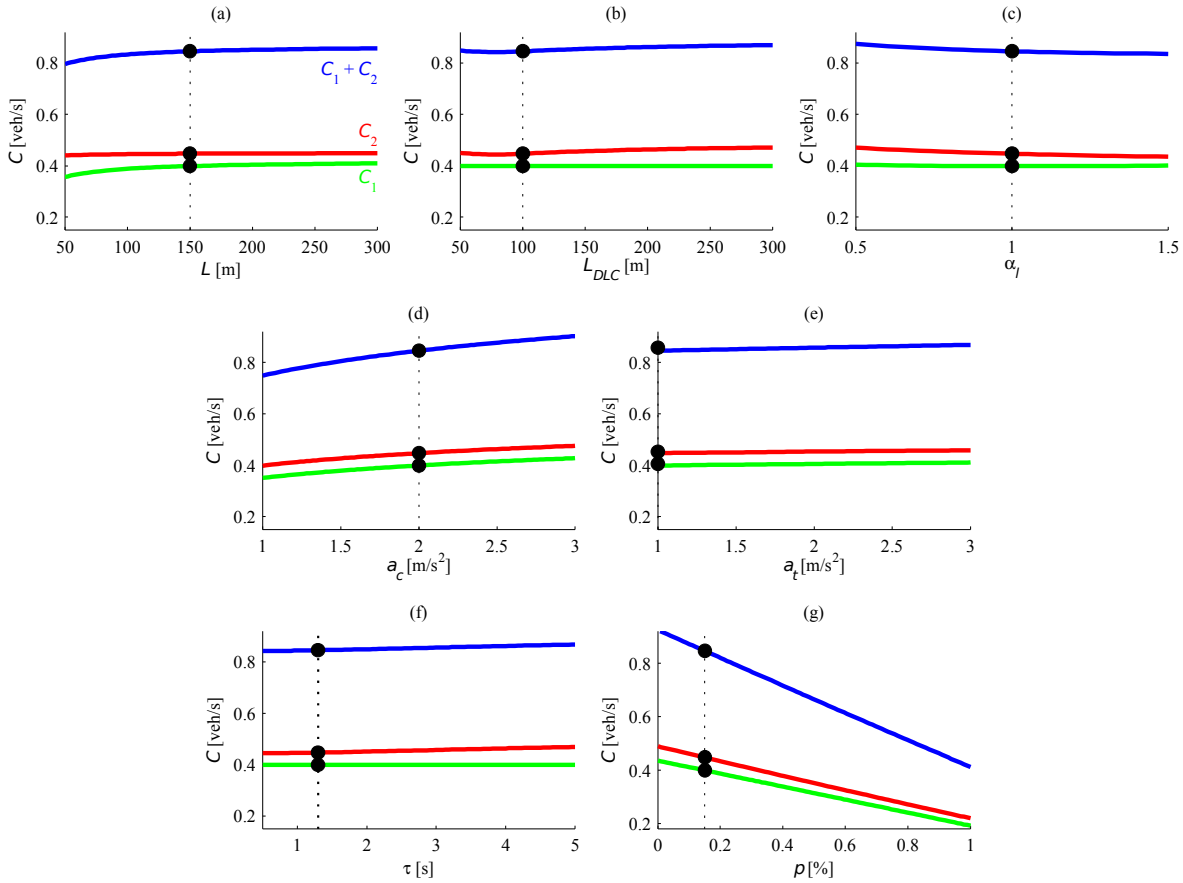

Figure 3: Sensitivity analysis to the different parameters (a) length of the on-ramp, L (b) length of the discretionary lane-changing area, L_{DLC} (c) local merge ratio, α_l (d) car acceleration, a_c (e) truck acceleration, a_t (f) time to complete a lane-changing maneuvers, τ (g) truck fraction, p.

Fig. 3d shows that the car acceleration significantly influences C_1 and C_2. C_1 increases from 0.35 to 0.41 veh/s (+17%) while C_2 increases from 0.4 to 0.46 veh/s (+15%) when a_c increases from 1 to 2.5 m.s^{-2}. The acceleration has been proven in (26) and (31) to be the most influential parameter for the effective capacity. This is confirmed here in a multilane context. Fig. 3e shows the influence of the truck acceleration. This influence looks limited but this is because the truck fraction is low, only 15 %. Thus, few trucks change lanes on average.

Fig. 3e presents the influence of duration of the discretionary lane-changing maneuvers. Obviously, this has no influence on C_1 because lane changes are mandatory for merge 1. C_2 increases from 0.44 to 0.46 veh/s (+5%) when τ increases from 1 to 4. Higher τ values mean that lane changes from lane 1 to lane 2 are harder, which leads to less severe capacity reduction on lane 2. Finally, Fig. 3f shows the

influence of truck fraction. As expected, the effective capacities on both lanes are very sensitive to this parameter.

Comparison with a multilane traffic simulator

The multilane analytical model entails an aggregate description of the lane-changing impacts. Furthermore, it neglects the relaxation effect that usually happens after vehicle insertion on the target lane (32), (36). Vehicles tend to accept shorter gap than the equilibrium (safe) one when changing lane and then progressively adapt their spacing with their leader. To test the relevance of the analytical formulae, it is interesting to compare the effective capacity per lane with the results provided by numerical simulations. Here, we use a microscopic traffic simulation based on Newell's model (37). This model is fully consistent with the kinematic wave theory when the fundamental diagram is triangular (33). Discretionary lane-changing rules correspond to the discrete formulation of the continuum model defined by Eq.(5), see (32) for details. A relaxation process is included after vehicle insertion. A constant speed difference equal to ε is maintained between a follower and its leader until reaching the equilibrium spacing, defined by the fundamental diagram, see also (32) for details. Mandatory lane changes are governed by Daganzo's model, see Eq.(2) and (2). In practice, the inserting rate is set to maintain on average a fixe local merge ratio between the on-ramp and the right lane. To ensure consistency between the numerical and the analytical results, discretionary lane changes are not allowed downstream of the on-ramp. We perform additional tests that relax this assumption in the numerical simulator and found little differences for the effective capacity values.

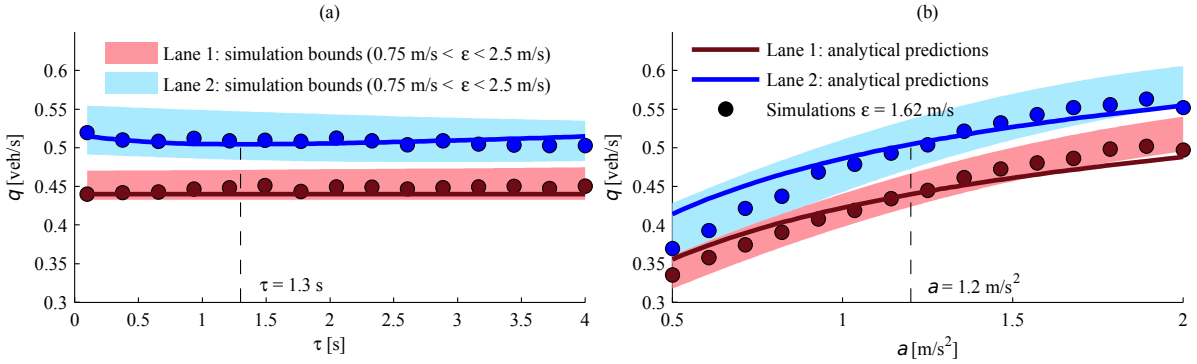

Figure 4: Comparison with simulation results (a) effective capacities for lanes 1 and 2 with respect to τ (b) effective capacities for lanes 1 and 2 with respect to a

Fig. 4 presents the comparison between the numerical (dots) and the analytical (lines) results for the reference scenario, but a single class of vehicles with a mean acceleration equal to 1.2 m.s^{-2}. The relaxation parameter is set to a classical value (32), i.e. ε=1.6 m.s^{-1}. Red plots correspond to the effective capacity for lane 1 while blue plots are related to lane 2. Fig. 4a tests different values for τ, the parameter related to the discretionary lane-changing process. Fig. 4b focuses on the most influential parameter for the capacity drop, i.e. the acceleration value a. Both figures highlight that the analytical formulae provide very good estimate for the effective capacity per lane when compared to the numerical results. Results are very close for all τ values. Results are close for a wide range of acceleration values, i.e. between 0.8 and 1.8 m.s^{-2}. Some discrepancies appear for very low or very high acceleration rate. A possible explanation is that the relaxation process induced lower speeds for followers that locally reinforce the capacity restrictions compared to the strict application of the moving bottleneck theory. Another possible explanation is that insertions in simulation are not necessarily uniformly distributed in space and time. The blue and red bands in Fig. 4b correspond to numerical simulations performed with lower (upper bound of the band) and higher (lower bound of the

bound) ε values. ε varies from 0.75 m.s^{-1} and 2.5 m.s^{-2}. This confirm our intuition because for low acceleration values, reducing the speed difference between inserting vehicles and their leaders lead to effective capacity values closer to the analytical estimation. A noticeable result is that whatever the acceleration value is the analytical estimation always falls within the band than corresponds to feasible ε values. Same result is observed in Fig. 4a.

We chose a traffic simulation with behavioral rules that are close to the behavioral assumptions of the analytical model because our purpose was to test if the local vehicle interactions resulting from traffic dynamics are well enough reproduced by the analytical model compared to a situation where all interactions are directly and properly considered. This test appears conclusive. We didn't try to compare the analytical model with a more complex traffic simulation and notably commercial one because to our best knowledge none has been proved to reproduce accurately the capacity drop phenomenon. For a more global proof, we prefer to resort to experimental observations as shown in the next section.

3. A first experimental validation

A first experimental validation is performed for a merge located on a southbound three-lane segment of the M6 highway near Manchester, UK (geographical coordinates: 53°25'14.85"N, 2°34'42.18"O). Fig. 5a proposes a sketch of the merge. Note that this is a UK freeway where vehicles drive on the left. A detector (M7072) is located 1600 m downstream of the merge. Two detectors are located just upstream (M7092) and downstream (M7088) of the merge. They provide flow and speed observations per lane every minutes. Inserting flows are calculated based on the difference of the total flow at these two stations with one-minute lag. This lag roughly represents the time that a vehicle needs to travel from M7092 to M7088 in congestion. All data from May 2006 is available. We picked up 6 business days where congestion is observed at the merge during the morning or the peak hours while loop M7072 experiments free-flow conditions. This guarantees that the merge is active (head of the queue). We only focused on heavy congestion where the speeds at M7088 and M7092 are below 50 km/h for all lanes. Finally, we have aggregated 1 min data over 20 min periods because our primary interest is to study the mean effective capacity values per lane. At the end, we have 17 sets of observations for loops M7092 and 7088 corresponding to 20 min of heavy congestion.

To perform the validation, we first need to extend the modeling framework to account for three lanes on the freeway. Fig. 5b shows how this can be straightforwardly implemented. A third merge between lane 2 and lane 3 is introduced upstream of the first two. This third merge accounts for the discretionary lane changes from lanes 2 to 3 and fulfills the non-overlapping condition with the other local merges. The length of the lane-changing areas for merges 2 and 3 are respectively denoted L^1_{DLC} and L^2_{DLC}. The third merge comes with two new unknowns: the lateral flow between lanes 2 and 3, q_{23} and the upstream flow on lane 3, q_3, and two equations: one similar to Eq.(7) that describes the flow exchange between lanes 2 and 3 and one similar to Eq.(3) that provides the effective capacity formulation C_3 for lane 3. We obtain a well-defined system with 6 equations and 6 unknowns that is solved using a numerical solver. Observations per lanes at M7088 are directly used to determine C_1, C_2 and C_3 values because this loop is just downstream of the merge. To estimate the values of q_1, q_2 and q_3, we start from the upstream observations Q_1, Q_2, Q_3 provided by loop M7092. By assuming that lane-changing maneuvers are only from the left to the right (from lane 1 to 2 or lane 2 to 3) it comes that $q_3=Q_3$, $q_2=Q_2-C_3+q_3$, $q_1=Q_1-C_2+q_2$.

The fundamental diagram for this experimental site has been calibrated in (38): w=19.4 km.h^{-1}, u=115 km.h^{-1} and κ=145 veh.km^{-1} per lane. The truck ratio p is set to 0. The maximal acceleration and the discretionary lane-changing duration are set to typical values without further calibration: a=1.8 m.s^{-2} and $\tau_1=\tau_2$=3 s. The length of the on-ramp L is 160 m. The lengths of the discretionary lane-changing areas L^1_{DLC} and L^2_{DLC} are both set to 100 m. This parameter has been shown to have little impacts on the effective capacities with the sensitivity analysis. Fig. 5c shows the experimental results for q_0 vs. q_1. Empty circles correspond to the 17 time periods while the red circle is the average over all the periods. This last observation is used to calibrate the local merge ratio, i.e. α_l=1.39. Fig. 5d presents the experimental results for C_2 vs. C_3. A noticeable point here is that the experimental distribution is uniform for all congested periods, i.e. $C_2 \approx C_3$.

Fig. 5e presents the result for the global validation, i.e. the relation between the on-ramp and the total upstream flows. It appears that the analytical model (green cross in Fig. 5e) provides a very close estimation of the total capacity, i.e. 5305 veh/h (-1.4%) compared to 5380 veh/h for the average of experimental observations (red circle). Furthermore, the global merge ratio α_g that results from the lane flow distribution predicted by the model is also very close to the real one, 0.22 compared to 0.2. This result is remarkable because as mentioned in the introduction previous analytical works (26) only provide very large upper and lower bounds for the total effective capacity in a multilane context, see brackets in Fig. 5e. Fig. 5c and Fig. 5d show that the analytical model also predicts extremely well the values of the effective capacities per lane: C_1=1545 veh.h^{-1}, C_2=1735 veh.h^{-1}, C_3=2026 veh.h^{-1}. The discrepancies compared to experimental values are respectively equal to -7%, -6% and +8.9%.

Finally, the blue shaded areas in Fig. 5c, Fig. 5d and Fig. 5e correspond to the results of the analytical model when the parameters vary within the following bounds: $0.5 \leq a \leq 2.5$ m.s^{-2}, $50 \leq L^1_{DLC} \leq 300$ m, $50 \leq L^2_{DLC} \leq 300$ m, $1 \leq \tau_1 \leq 5$ s, $1 \leq \tau_2 \leq 5$ s, $1 \leq \alpha_l \leq 2$. Almost all the experimental observations for the different congestion periods fall within the blue shaded areas in all figures. This ends the demonstration of the performance of the analytical model for this experimental merge because this highlights that the analytical model can fit all individual observations with feasible parameter values.

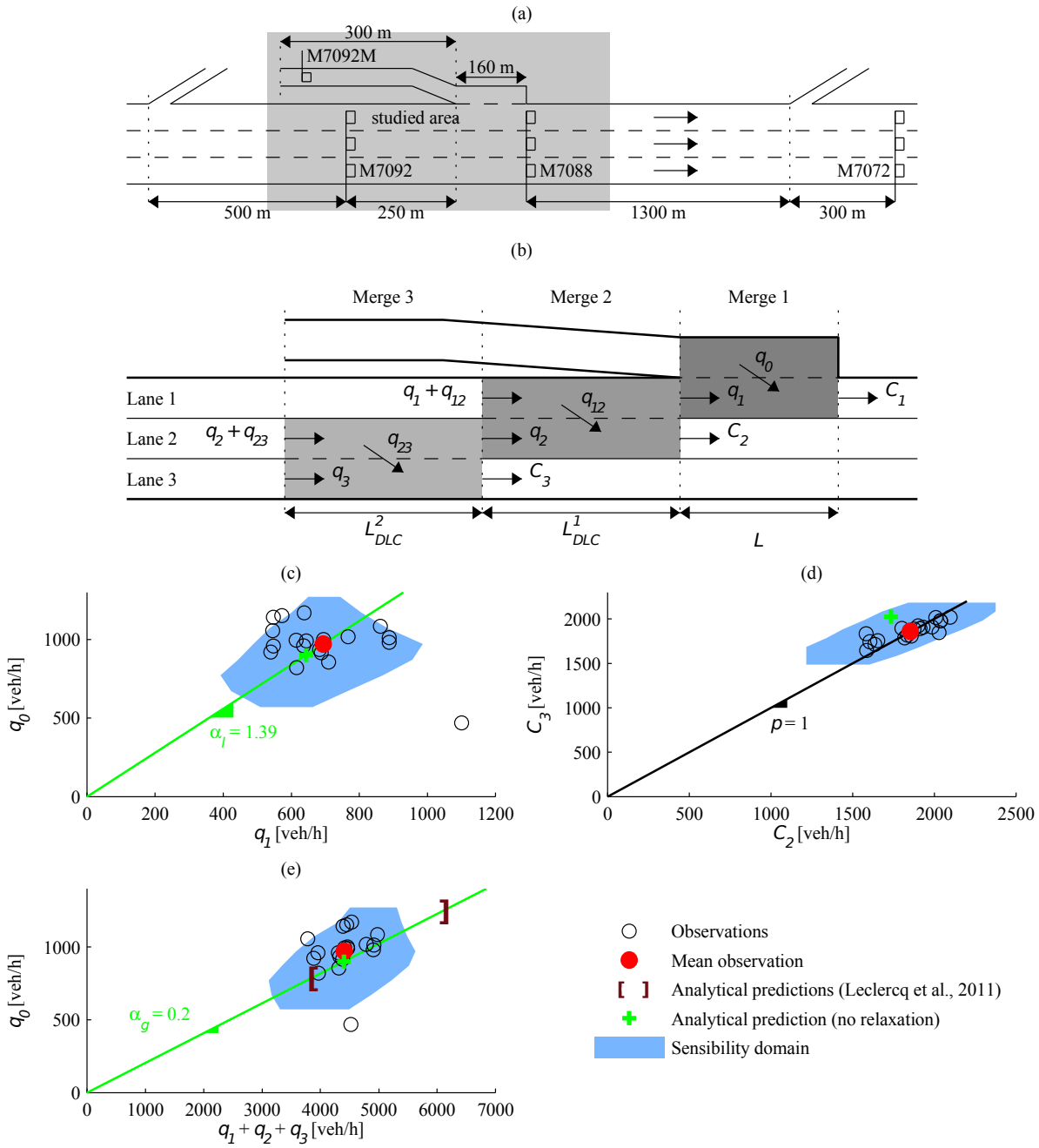

Figure 5: Experimental validation (a) Sketch of the experimental site (b) Partitioning lane-changing maneuvers for a three-lane freeway (c) Inserting flow vs. right lane flow (d) Center vs. left lane effective capacity (e) Inserting flow vs. total effective capacity

4. Conclusion

This paper proposes an analytical framework to estimate the capacity drop when multilane freeway merges act as active bottlenecks. This framework provides first order approximations of the mean effective capacity for all lanes. We showed that these estimations are consistent with the results obtained from a traffic simulator that fully describe vehicle interactions. More important, we demonstrated on a first experimental site that the estimations fit very well with empirical observations during heavy congestion.

The formulation of the analytical model as a system of equations may look complex but it provide instantaneous solution when implemented as a script combined with a numerical solver. There is no need to replicate a huge number of simulation runs like with traffic simulators or to analyze long-term on-field data time series to identify congestion periods. This formulation can be used to design new merges or to refine real-time traffic estimation model using updated capacity formulation for merges. More important sensitivity analyses are straightforward, which helps to clearly identify the most influential factors and to shed light on how the different local phenomenon and notably the different kinds of lane changes influence the effective capacity values per lane and in total.

Further researchers are needed to validate the model on a large set of different experimental site with different configurations (number of lanes, length of the on-ramp,…). With the inputs of (34) it would be easy to account for different truck ratios per lane and further refined the system. Finally, it is important to mention that this paper provides the first analytical connection between the local and the global merge ratio. (6) investigates such a connection from an experimental perspective focusing on the lane flow distribution. Here the macroscopic lane flow distribution is an output of the analytical model and results from an averaging process of local phenomenon. This may help to better understand traffic behavior at merges and improve control algorithms.

Acknowledgements

The authors are grateful to the Highways Agency of England for providing data on M6 freeways. This research is partly sponsored by the NWO project "There is plenty of room in the other lane".

References

(1) Newell, G.F. Applications of the queueing theory (2nd edition). New York: cahpman & Hall, 303 p.

(2) Daganzo, C. The cell transmission model, Part II: network traffic. *Transportation Research Part B*, 29(2), 1995, pp. 79-93.

(3) Bar-Gera, H., and S. Ahn. Empirical macroscopic evaluation of freeway merge-ratios. *Transportation Research Part C*, 18, 2010, pp. 457-470.

(4) Troutbeck, R.J. The performance of uncontrolled merges using a limited priority process. In: Taylor, M.A.P., (Ed.), *Proceedings of the 15th International Symposium on Transportation and Traffic Theory*, Amsterdam: Pergamon, 2002, pp. 463-482.

(5) Cassidy, M.J and S. Ahn. Driver turn-taking behavior in congested freeway merges. *Transportation Research Record - Journal of the Transportation Research Board*, No.1934, 2005, pp. 140-147.

(6) Reina, P. and S. Ahn. Prediction of merge ratios using lane flow distributions. 2015, *under review*.

(7) Yuan, K., Knoop, V.L. and P. Hoogendoorn. Capacity Drop: A relation between the speed in congestion and the queue discharge rate, *Transportation Research Board Annual Meeting 2015*, #15-4064, 2015, 17 p.

(8) Cassidy, M.J. and R.L. Bertini. Some traffic features at freeway bottlenecks. *Transportation Research Part B*, 33(1), 1999, pp. 25-42.

(9) Hall, F.L and K. Agyemang-Duah. Freeway Capacity Drop and The Definition of Capacity. *Transportation Research Record - Journal of the Transportation Research Board*, No.1320, 1991, 8 p.

(10) Elefteriadou, L., Roess, R.P. and W.R. McShane. Probabilistic nature of breakdown at freeway merge junctions. *Transportation Research Record - Journal of the Transportation Research Board*, No.1484, 1995, pp. 80-89.

(11)Persaud, B., Yagar, S. and R. Brownlee. Exploration of the Breakdown Phenomenon in Freeway Traffic. *Transportation Research Record - Journal of the Transportation Research Board*, No.1634, 1998, pp. 64-69.

(12) Chung, K., Rudjanakanoknad, J. and M.J. Cassidy. Relation between traffic density and capacity drop at three freeway bottlenecks. *Transportation Research Part B*, 41(1), 2007, pp. 82-95.

(13) Sarvi, M., Kuwahara, M. and A. Ceder. Observing freeway ramp merging phenomena in congested traffic. *Journal of Advanced Transportation*, 41(2), 2007, pp. 145-170.

(14) Oh, S. and H. Yeo. Estimation of Capacity Drop in Highway Merging Sections. *Transportation Research Record - Journal of the Transportation Research Board*, No.2286, 2012, pp. 111-121.

(15) Srivastava, A. and N. Geroliminis. Empirical observations of capacity drop in freeway merges with ramp control and integration in a first-order model. *Transportation Research Part C*, 30, 2013, pp. 161-177.

(16) Zheng, Z.*, Ahn, S., Chen, D., Hourdos, J., Capacity drop at freeways: new observations and statistical modeling. 21st International Symposium of Transportation and Traffic Theory. *under review*.

(17) Cassidy, M.J., and J., Rudjanakanoknad. Increasing capacity of an isolated merge by metering its on-ramp, *Transportation Research Part B*, 39(10), 2005, pp. 896-913.

(18) Laval, J.A., M.J. Cassidy, and C.F. Daganzo. Impacts of lane changes at on-ramp bottlenecks: a theory and strategies to maximize capacity. In: R. Kühne, T. Poeschl, T., A. Schadschneider, M. Schreckenberg, D. Wolf (Eds.), *Traffic and Granular Flow '05'*. Berlin: Springer, 2005, pp. 577-586.

(19) Treiber, M., A. Kesting, and D. Helbing. Understanding widely scattered traffic flows, the capacity drop, and platoons as effects of variance-driven time gaps, *Phys. Review E*, 74(2), 2006, pp. 1-10.

(20) Laval, J.A., and C.F. Daganzo. Lane-changing in traffic streams, *Transportation Research Part B*, 40(3), 2006, pp. 251-264.

(21) Coifman, B., and S. Kim. Extended Bottlenecks, the Fundamental Relationship and Capacity Drop. *Transportation Research Part A*. 45(9), 2011, pp. 980-99.
(22) Chen, D., S. Ahn, J.A. Laval, and Z. Zheng. On the periodicity of traffic oscillations and capacity drop: the role of driver characteristics, *Transportation Research Part B*, 59, 2014, pp. 117-136.
(23) Carlson, R.C., Papamichail, I. and M. Papageorgiou,. Integrated feedback ramp metering and mainstream traffic flow control on motorways using variables speed limits. *Transportation Research Part C*, 46, 2014, pp. 209-221.
(24) Coifman, B. and S. Kim. Extended bottlenecks, the fundamental relationship, and capacity drop on freeways. *Transportation Research part A*, 45(9), 2011, 980-991.
(25) Kim, S. and B. Coifman. Driver relaxation impacts on bottleneck activation, capacity, and the fundamental relationship. *Transportation Research part C*, 36, 2013, pp. 564-580.
(26) Leclercq, L., J.A. Laval, and N. Chiabaut. Capacity Drops at Merges: an endogenous model, *Transportation Research Part B*, 45(9), 2011, pp. 1302-1313.
(27) Newell, G.F. A moving bottleneck. *Transportation Research Part B,* 32(8), 1998, pp. 531-537.
(28) Leclercq, L., S. Chanut, and J.B. Lesort. Moving bottlenecks in the LWR model: a unified theory, *Transportation Research Record: Journal of the Transportation Research Board*, No.1883, 2004, pp. 3-13.
(29) Lighthill, M.J., and J.B. Whitham. On kinematic waves II: A theory of traffic flow in long crowded roads, *Proceedings of the Royal Society*, A229, 1955, pp. 317-345.
(30) Richards, P.I. "Shockwaves on the highway". *Operations Research*, 4, 1956, pp. 42-51.
(31) Leclercq, L., Knoop, V.L., Marczak, F. and S.P. Hoogendoorn. Capacity drops at merges: new analytical investigations. *Transportation Research part C*, 2015, *under review*.
(32) Laval, J.A. and L. Leclercq. Microscopic modeling of the relaxation phenomenon using a macroscopic lane-changing model. *Transportation Research Part B*, 42(6), 2008, pp. 511-522.
(33) Daganzo, C.F. A variational formulation of kinematic waves: basic theory and complex boundary conditions, *Transportation Research Part B*, 39(2), 2005, pp. 187-196.
(34) Leclercq, L., Knoop, V.L., Marczak, F. and S.P. Hoogendoorn. Capacity drops at merges: new analytical investigations. *Proceedings of the 17th International IEEE Conference on Intelligent Transportation Systems*, Qingdao, China, October 8-11, 2014, 6 p.
(35) Marczak, F., Leclercq, L. and C. Buisson. A Macroscopic Model for Freeway Weaving Sections. *Computer-Aided Civil and Infrastructure Engineering*, 30(6), 2015, pp. 464-477.
(36) Hidas, P. Modelling vehicle interactions in microscopic simulation of merging and weaving. *Transportation Research Part C*, 13, 2015, pp. 37–62.
(37) Newell, G.F. A simplified car-following theory: a lower order model. *Transportation Research Part B*, 36(3), 2002, pp. 195-205.
(38) Chiabaut, N., Leclercq, L., Bretin, T. and C. Buisson. Calibrating the Fundamental Diagram in Congestion: Methods Based on Observations at Consecutive Loop-Detectors. *Proceedings of the IWTDCS Conference, 8-9 September, Barcelona, (Spain)* Tokyo: University of Tokyo, 2008, 9 p.